ORNL/TM-2021/2247

FY21 Progress Report on Graphite-Salt Interaction Studies

Nidia C. Gallego
Cristian I. Contescu
James R. Keiser
Jun Qu
Xin He
Kristian Myhre

September 2021

Approved for public release.
Distribution is unlimited

OAK RIDGE National Laboratory

ORNL IS MANAGED BY UT-BATTELLE LLC FOR THE US DEPARTMENT OF ENERGY

ORNL/TM-2021/2247

Chemical Sciences Division

FY21 PROGRESS REPORT ON GRAPHITE-SALT INTERACTION STUDIES

Nidia C. Gallego
Cristian I. Contescu
James R. Keiser
Jun Qu
Xin He
Kristian Myhre

September 2021

Prepared by
OAK RIDGE NATIONAL LABORATORY
Oak Ridge, TN 37831-6283
managed by
UT-BATTELLE LLC
for the
US DEPARTMENT OF ENERGY
under contract DE-AC05-00OR22725

CONTENTS

LIST OF FIGURES

LIST OF TABLES

ABSTRACT

This report summarizes the activities performed in FY21 to investigate the interactions between nuclear graphite and molten salts, such as FLiNaK. First, building on last year's achievements, the team improved the procedure for measurements on pressurized salt intrusion in nuclear graphite and performed new experiments at variable pressures with specimens of different sizes and shapes. Additionally, the team actively provided suggestions and comments for ASTM D8091, *Standard Guide for Impregnation of Graphite with Molten Salts*, which came up for periodic revision in 2021. Second, the team expanded its capabilities to further characterize salt-impregnated graphite by procuring and installing a laser-induced breakdown spectroscopy (LIBS) instrument capable of producing a 3D chemical composition of a surface and subsurface region of specimens. A methodology for accurately analyzing information was developed, and a manuscript was submitted for publication. The LIBS instrument sample cell is sealed in controlled inert atmosphere, which is an advantage for using humidity-sensitive samples and Be-contaminated samples. This aligns with the team's effort to expand the capabilities of handling FLiBe and Be-containing materials in two newly installed glovebox units. Third, the team performed preliminary tribology tests for pebble graphite wear in contact with stainless steel in dry state and in molten salt at high temperature. These tests are needed to establish the baseline for the wear of pebble graphite by friction against metallic walls. The friction and wear of pebbles in the fluoride salt-cooled high-temperature reactor are expected to generate dust, which is a concern for other components' properties and safe reactor operation.

1. UPDATE ON GRAPHITE SALT INTRUSION STUDIES

In continuation of last year's studies on molten salts intrusion in graphite, during FY21, the team improved the experimental procedure for graphite impregnation in pressurized FLiNaK at 750°C. Additional intrusion experiments were performed to monitor the effect of the impregnation pressures, and capabilities for the surface characterization of salt-impregnated graphite materials were developed. To this aim, the team procured and installed a laser-induced breakdown spectroscopy (LIBS) instrument and performed initial runs to optimize the standard data collection procedure.

1.1 EXPERIMENTAL SET UP AND TESTS

The experimental setup built specially for salt intrusion experiments was presented in detail in a previous report.[1] The main section of the high-pressure salt-infiltration rig (Figure 1) consists of the graphite-lined containment vessel, which protects the molten salt from contact with metals, and the all-graphite sample holder, which accommodates up to six graphite specimens. The sample holder design allows for unrestricted salt access to vertical surfaces of graphite specimens and most horizontal surfaces supported by the sample holder. The long graphite extension rod that connects with the sample holder can be moved vertically to immerse or remove the sample holder from the molten salt at the bottom of the containment vessel. On the top of the containment vessel, the high-pressure rig is divided in two sections separated by a full port ball valve. The bottom section connects directly with the containment vessel, and the upper section allows graphite samples to be temporarily stored and isolated from the environment above the molten salt. Connections to the piping system allow each section to be independently evacuated, flushed, or pressurized with inert gas.

[1] N. C. Gallego, C. I. Contescu, and J. Keiser, *Progress Report on Graphite-Salt Intrusion Studies*, ORNL/TM-2020/1621 (2020).

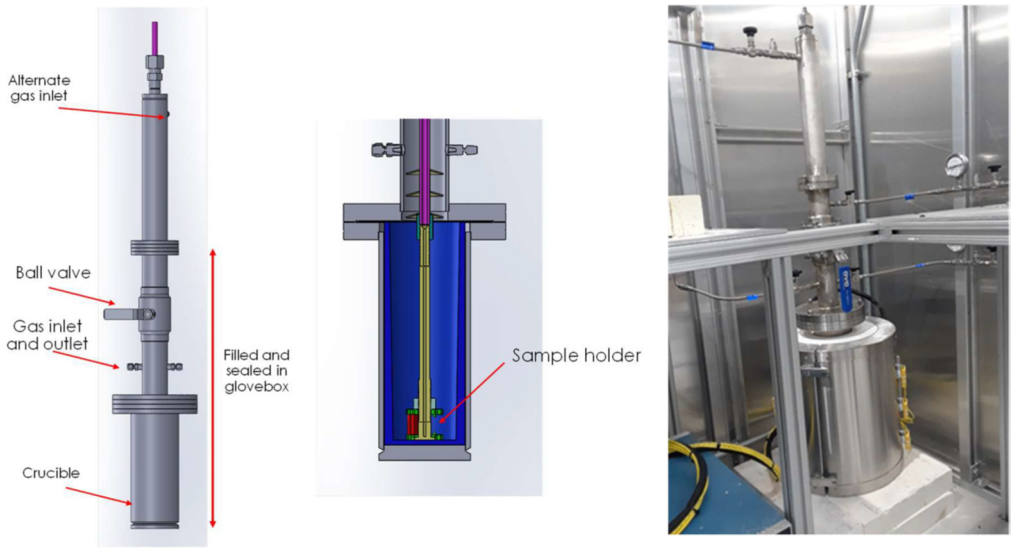

Figure 1. The salt-intrusion rig for graphite exposure to high-pressure molten salt intrusion.

The system was designed according to the guidelines of ASTM D8091-21[2] and can operate at temperatures up to 750°C and pressures up to 1 MPa. According to the procedures recommended by this standard guide, graphite specimens of predetermined shape and size were laser-marked, dried, weighed, and then stored in a desiccator for future use. In preparation for intrusion experiments, the specimens and graphite sample holder were outgassed in high vacuum at 1,200°C. After mounting the specimens in the sample holder, the assembly was loaded and kept in a rough vacuum above the ball valve, and the salt containment compartment was continually flushed with Ar while the temperature was gradually raised to melt the salt. After thermal equilibration at the desired temperature, the ball valve was opened, and the specimens were lowered above the molten salt level. Two different settings were selected for specimens' initial condition before immersing in the molten salt: in flowing Ar at near-atmospheric pressure ($P_0 \approx$ 100 kPa) or from a rough vacuum ($P_0 \approx 0$ kPa). After immersing the specimens in the salt, the system was sealed, and the Ar gas pressure was raised to the desired level (P_1). After 12 h, the samples were raised above the salt level, and the system was cooled overnight while maintaining the Ar pressure. In other instances, the pressure was released before allowing the system to cool, and the system was flushed with Ar at near-atmospheric pressure. Before opening the system after cooling, the samples were raised above the ball valve, and the valve was closed to protect the salt under an Ar blanket. The specimens were carefully transferred to an Ar glove box for weighing and storage. Removing samples from the holder was sometimes difficult because of residual salt solidification around samples.

Table 1 shows the structural and porosity properties of various graphite grades studied. Six different FLiNaK impregnation campaigns were started in 2019. The graphite grades studied thus far can be classified as *superfine* (IG-110, 2114, and ETU-10), *fine* (NBG-25), and *medium-fine* (PCEA and NBG-18) according to ASTM D8075.[3] One more test was done with graphite CGB, specially manufactured and used for the Molten Salt Reactor Experiment (MSRE) project at Oak Ridge National Laboratory (ORNL). The specimens used for impregnation were machined either as rectangular prisms ($12.7 \times 12.7 \times 25$ mm^3) or right cylinders (10 mm Φ × 20 mm H). The corresponding surface-to-volume ratios of the two geometries were 3.28 for prisms and 3.0 for cylinders.

[2] ASTM D8091-21, *Standard Guide for Impregnation of Graphite with Molten Salts*, ASTM International, West Conshohocken, Pennsylvania, www.astm.org.
[3] ASTM D8075-16, *Standard Guide for Categorization of microstructural and Microtextural Features Observed in Optical Micrographs of Graphite*, ASTM International, West Conshohocken, Pennsylvania, www.astm.org.

Table 1. Microstructural and porosity properties of graphite grades used on intrusion studies.

Graphite grade	Classification [a]	Grain size [b]	Bulk density [c]	Skeleton density [d]	Specific volume of open pores [e]	Specific volume of closed pores [f]	Specific total pore volume [g]	Porosity [h]	Pore opening diameter [i]
		mm	$g \cdot cm^{-3}$	$g \cdot cm^{-3}$	$cm^3 \cdot g^{-1}$	$cm^3 \cdot g^{-1}$	$cm^3 \cdot g^{-1}$	%	mm
IG-110	superfine	10	1.76	2.05	0.079	0.041	0.12	21	3.9
2114	superfine	13	1.81	2.08	0.071	0.034	0.105	19	3.5
ETU-10	superfine	15	1.74	2.10	0.098	0.031	0.129	22	3.6
NBG-25	fine	60	1.81	2.07	0.068	0.038	0.105	19	5.1
PCEA	medium-fine	800	1.77	2.00	0.065	0.054	0.119	21	64
NBG-18	medium-coarse	1,600	1.86	2.02	0.044	0.048	0.092	17	18
CGB	medium-fine	N/A	1.86	1.87	0.003	0.089	0.091	17	0.2

Notes:
[a] Classification according to ASTM D8075-16[3]
[b] Based on manufacturer's information. No information was found for grade CGB. Information on grade NBG-25 from Chi, Kim, and Jang.[4]
[c] Data from physical measurements according to ASTM C559-16.[5]
[d] Data from He pycnometry according to ASTM B923-20.[6]
[e] Calculated as $\left[\frac{1}{\rho_{bulk}} - \frac{1}{\rho_{skelet}}\right]$.
[f] Calculated as the difference between total pore volume and open pore volume.
[g] Calculated as $\left[\frac{1}{\rho_{bulk}} - \frac{1}{2.24}\right]$.
[h] Calculated as $V_t \times \rho_{bulk} \times 100\%$.
[i] From Hg porosimetry.

1.2 RESULTS AND DISCUSSION

Figure 2 summarizes the FLiNaK intrusion results obtained thus far for the several graphite grades, which are shown as discrete data points. Intruded salt volumes (cm^3 salt/g graphite) were measured after exposure to molten FLiNaK for 12 h at 750°C. The intrusion pressure (ΔP) was varied between 5 and 7 bar. The intrusion pressure is defined as $\Delta P = P_1 - P_0$, where P_0 is the starting pressure above the molten salt before lowering the graphite samples, and P_1 is the Ar overpressure above the molten salt measured by the pressure gauge. The figure also shows Hg intrusion porosimetry data (cm^3 Hg/g graphite) plotted on the pressure-shifted scale that converts Hg penetration pressures into FLiNaK penetration pressures at 750°C:[1]

$$\log \Delta P_{FLiNaK} = \log \Delta P_{Hg} + \log\left(\frac{\gamma_{FLiNaK} \cos \theta_{graphite/FLiNaK}}{\gamma_{Hg} \cos \theta_{graphite/Hg}}\right). \quad (1)$$

[4] S.-H. Chi, G.-C. Kim, and J.-H. Jang, "Effects of the Air Flow Rate on the Oxidation of NBG-18 and 25 Nuclear Graphite Grades, Trans. Korean Nuclear Society Spring Meeting, Jeju, Korea, May 10–11, 2007.
[5] ASTM C559-16, *Standard Test Method for Bulk Density by Physical Measurements of Manufactured Carbon and Graphite Articles*, ASTM International, West Conshohocken, Pennsylvania, www.astm.org.
[6] ASTM B923-20, *Standard Test Method for Metal Powder Skeletal Density by Helium or Nitrogen*, ASTM International, West Conshohocken, Pennsylvania, www.astm.org.

In this equation, γ is the surface tension (0.169 N/m for FLiNaK at 750°C and 0.485 N/m for Hg at 25°C),[7,8] and θ is the wetting angle (135° for FLiNaK on graphite IG-110 at 750°C and 155° for Hg on graphite IG-110).[7,9,10]

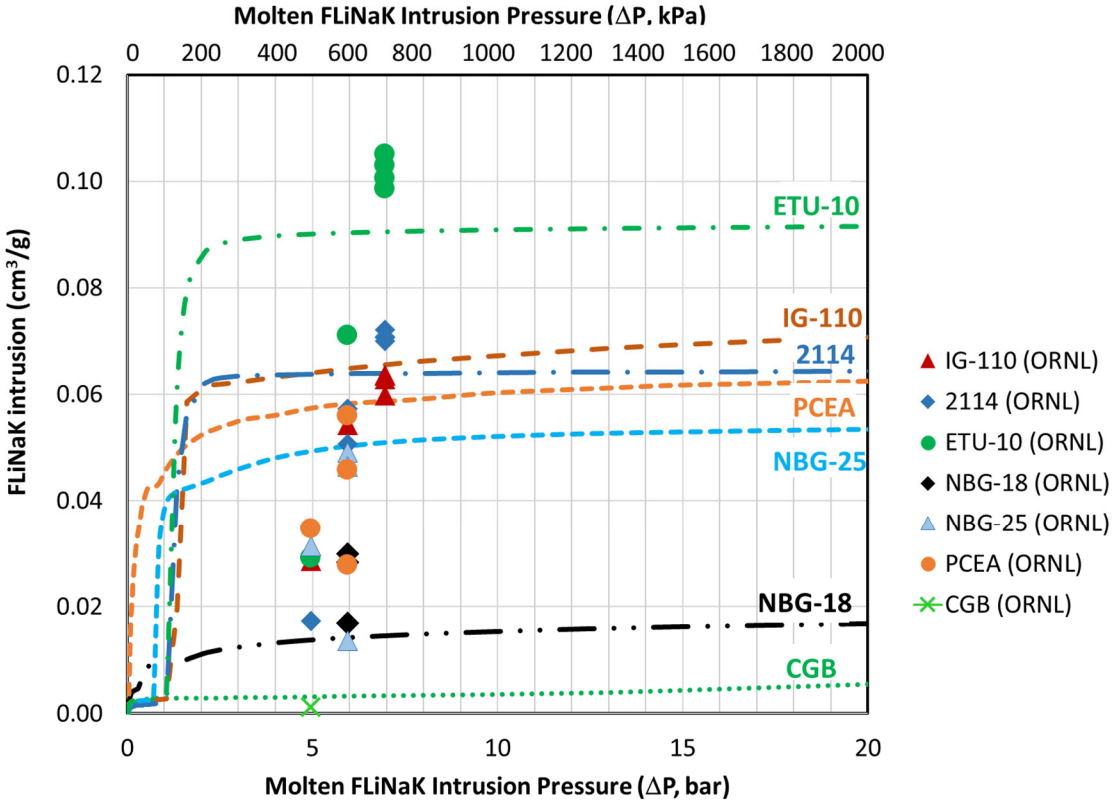

Figure 2. The amount of intruded FLiNaK vs. intrusion pressure (*ΔP*) after 12 h exposure at 750°C along with predicted intrusion behavior vs. FLiNaK pressure based on Hg porosimetry results.

As shown in Figure 2, all pressures selected for FLiNaK impregnation were above the threshold impregnation pressures characteristic for each graphite grade. The threshold impregnation pressure for FLiNaK is the equivalent of the abrupt increase (i.e., percolation) of intruded Hg volume obtained from Hg porosimetry[1] after converting pressure scales using Eq. (1). For the graphite grades investigated, the threshold pressures for molten FLiNaK infiltration, ΔP_{FLiNaK}, were between 1 and 2 bar (100–200 kPa) and even below 1 bar for PCEA. *ΔP* is not the absolute pressure at salt percolation but the difference between the pressurized salt environment and the initial pressure in graphite pores before immersion.

[7] M. S. Sohal, M. A. Ebner, P. Sabharwall, and P. Sharpe, *Engineering Database of Liquid Salt Thermophysical and Thermochemical Properties*, INL/EXT-10-18297 (2013), https://inldigitallibrary.inl.gov/sites/sti/sti/5698704.pdf.
[8] ASTM D4284-12, *Standard Test Method for Determining Pore Volume Distribution of Catalysts by Mercury Intrusion Porosimetry*, ASTM International, West Conshohocken, Pennsylvania, (2017), www.astm.org.
[9] A. R. Delmore, W. Derdeyn, R. Gakhar, and R. O. Scarlat, "Wetting of Graphite by Molten Fluoride Salts: Initial Experiments," *Trans. American Nucl. Soc.* 118 (2018): 121–124.
[10] Z. He, L. Gao, W. Qi, B. Zhang, X. Wang, J. Song, X. He, C. Zhang, H. Tsang, R. Holmes, H. Xu, and X. Zhou, "Molten FLiNaK Salt Infiltration into Degassed Nuclear Graphite under Inert Gas Pressure," *Carbon* 84 (2015): 511–518.

ASTM D8091-21 introduced the parameter D_0 to represent the volumetric fraction of open pores in a given graphite specimen intruded by salt at the experimental conditions:

$$D_o = \frac{W_2 - W_1}{\rho_{\text{FLiNaK}} V_0} \quad (2)$$

In this equation, W_1 and W_2 are the mass of graphite specimens before and after salt impregnation, respectively; ρ_{FLiNaK} is the molten FLiNaK density at the impregnation temperature (1.982 g/cm^3 at 750°C)[7]; and V_o is volume of open pores (cm^3) in a given graphite sample. The latter is calculated from the apparent (i.e., bulk) graphite density obtained from physical measurements according to ASTM C559--21[5] and the skeletal density of graphite. Because a standard method specific to nuclear graphite is unavailable, the skeletal density was measured according to the He pycnometry method in ASTM B923-20 designed for metal powders.[6]

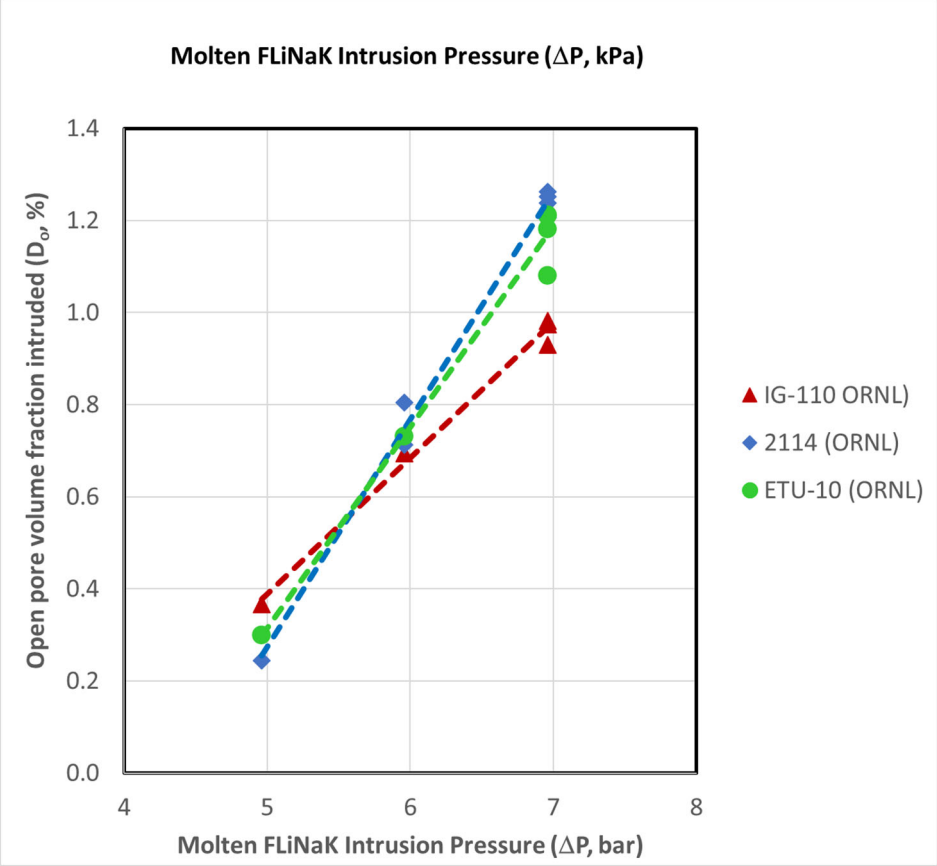

Figure 3. Effect of intrusion pressure on the fraction of open-pore volume intruded by FLiNaK at 750°C.

Figure 3 shows the results for superfine grades IG-110, 2114, and ETU-10 for which more data were available. With the increase of impregnation pressure, the fraction of open-pore volume impregnated by FLiNaK increases almost linearly with pressure but with different rates for each graphite. The differences could be attributed to limitations caused by friction[11] correlated with the pore structure (e.g., tortuosity, pore connectivity) of each graphite grade. IG-110 has the slowest rate of increase, showing that its structure develops higher opposition to dynamic salt intrusion. Moreover, D_o is expected to tends toward

[11] W. P. Eatherly et al., "Physical Properties of Graphite Materials for Special Nuclear Applications," *Proceedings of 2nd United Nations International Conference on the Peaceful Uses of Atomic Energy*, Geneva, 1938, vol 7 (United Nations, New York, 1959): 389–401.

unity when all open pores available before impregnation are filled by intruded salt. This is observed for IG-110 but not for 2114 and ETU-10, where $D_o > 1$. This deviation might be due to inherent measurement errors in the He pycnometry method. An alternate explanation would be that the measuring pressure was high enough for the infiltrated salt to create access to the closed pores that are always present in graphite. In this case, ASTM D8091-21 recommends an alternate parameter (D_t) for the fraction of total pore volume infiltrated by salt:

$$D_t = \frac{w_2 - w_1}{\rho_{\text{salt}} V_t}, \tag{3}$$

where V_t is the total open and closed pore volume calculated from the apparent graphite density, the density of perfect graphite crystals (2.24 g/cm^3), and the mass of the given sample.

At this point, the available data are limited and insufficient to determine the effect of the sample size and geometry on the calculated D_0 and D_t parameters. This is a significant limitation of ASTM D8091-21.[2] This standard guide provides good recommendations for performing reproducible and consistent measurements of pressurized intrusion of molten salts in graphite combined with an evaluation of the pore volume fraction occupied by intruded salts. However, ASTM D8091 does not recommend a standard size and shape of graphite specimens, which are important experimental factors properly accounted for and standardized by methods D7542[12] and C1179[13] for graphite oxidation. That makes it difficult to compare results between various groups, to ascertain specific infiltration behavior of graphite materials, and to rank graphite grades as a function of their infiltration resistance in standard conditions. Similarly, ASTM D8091 does not recommend the duration of molten salt exposure. The amount of impregnated salt increases with time for some graphite grades but not all.[9] The rate of pressurized liquid penetration inside the pore system depends on pore connectivity, which is an intrinsic property of each graphite relevant to the salt impregnation behavior.

1.3 CHARACTERIZATION OF SALT-EXPOSED GRAPHITE SAMPLES

Graphite was selected as a moderator in contact for the MSRE project because it has a much higher compatibility with molten salts at high temperature and under neutron irradiation than any available corrosion-resistant alloys. First assessments of MSRE results were that graphite's resistance to salt interactions (FLiBe with or without added fuel) was better than expected.[14] However, post-experiment examinations of graphite moderator samples extracted after 9 months of reactor operation produced new information. Prompt irradiation measurements after proton bombardment in the ORNL van de Graaff accelerator detected 100 times more Li and F in irradiated graphite moderator than in the unirradiated graphite. The penetration depth in irradiated sample (500 μm) was higher than in unirradiated material (200 μm), indicating that enhanced ionic diffusion in the irradiated graphite was in contact with the hot fueled salt.[15]

More recent investigations that used advanced surface characterization methods detected stronger than expected interactions between nuclear graphite and molten fluoride salts. Graphite reacts with F gas and some F compounds (e.g., ClF_3, BrF_3, XeF_2, LiF) to form graphite fluorine intercalation compounds

[12] ASTM D7542, *Standard test Method for Air Oxidation of Carbon and Graphite in the Kinetic Regime*, ASTM International. West Conshohocken, Pennsylvania, www.astm.org.
[13] ASTM C1179, *Standard Test Method for Oxidation Mass Loss of Manufactured Carbon and Graphite Materials in Air*, ASTM International. West Conshohocken, Pennsylvania, www.astm.org.
[14] P. N. Haubenreich and J. R. Engel, "Experience with the Molten-Salt Reactor Experiment," *Nuclear Applications & Technology* 8 (1970): 118–136.
[15] R. L. Macklin, J. H. Gibbons, E. Ricci, T, Handley, and D. Cuneo, "Proton Reaction Determination of Lithium and Fluorine in Molten Salt Reactor Graphite," *Nuclear Applications* 5 (1968): 269.

$(CF_x)_{0<x<1}$.[16] Although both FLiBe and FLiNaK are high-temperature ionic liquids, the F ion activity is different. In FLiBe (molar ratio of 2 LiF : 1 BeF_2), most free F^- ions are bonded in the $[BeF_4]^{2-}$ ion (tetrafluoroberyllate).[17] In FLiNaK, all F^- ions are free, and they can aggressively react with graphite.

It has been predicted that F^- ions can interact with surface defect sites in graphite[18] and can substitute terminal H atoms at edge sites of graphene layers. Forming new C–F bonds accompanied by local graphite lattice expansion was detected on IG-110 graphite after immersion in molten FLiNaK for 16 h at 500°C.[19] Surprisingly, surface fluorination was also detected on IG-110 graphite after 12 h contact with FLiBe at 700°C.[20] In the latter case, subsurface penetration of F was higher than that of Li and Be. Moreover, fluorination induced local changes in graphite microstructure, such as an increase of rhombohedral phase content and sp^3 hybridized C atoms.[9] This local structural change could create new trapping sites for tritium retention in graphite materials exposed to fluoride salts,[21] as suggested by post-experiment examinations of graphite materials extracted from the MSRE reactor after 5 years of contact with molten salt.[22]

LIBS is a useful technique for providing spatially resolved chemical composition information for graphite samples exposed to molten fluoride salts. This technique operates by focusing a light beam from a high-power pulsed laser strong enough to cause the localized optical breakdown of the target material and the formation of a plasma. Excited species in the plasma, mostly neutral and ionic single atom species, de-excite and produce optical emission spectra that characterize a sample's composition. The LIBS technique is very useful and convenient for producing elemental depth profiling and mapping.[23]

To explore the surface composition of graphite samples exposed to FLiNaK, a J200-ns LIBS instrument was procured from Applied Spectra. The instrument uses a Nd:YAG laser operating at a 266 nm wavelength. A sealable sample holder allows for position control and operation in controlled gas environment (i.e., protected from moisture and oxidation). This feature will make possible the future analysis of graphite samples exposed to molten FLiBe, which is toxic. Figure 4 shows the LIBS instrument along with the sealed sample holder and a close view of the latter with graphite specimens in place.

---

[16] M. Inagaki, "New Carbons. Control of structure and functions," *Elsevier* 2000, Chapter 6, "Intercalation Compounds."
[17] S. Liu, T. Su, J. Cheng, X. An, P. Zhang, H. Liu, S. Yao, L. Xie, and H. Hou, "Investigation on Molecular Structure of Molten Li_2BeF_4 (FLiBe) Salt by Infrared Absorption Spectra and Density Functional Theory," *J. Molecular Liquids* 242 (2017): 1052–1057.
[18] S. Wang, X. Ke, W. Zhang, W. Gong, P. Huai, W. Zhang, and Z. Zhu, "Fluorine Interaction with Defects on Graphite Surface by a First-Principles Study," *Applied Surface Science* 292 (2014): 488–493.
[19] X. Yang, S. Feng, X. Zhou, H. Xu, and T. K. Sham, "Interaction between Nuclear Graphite and Molten Fluoride Salts: A Synchrotron Radiation Study of the Substitution of Graphitic Hydrogen by Fluoride Ion," *Journal of Physical Chemistry A* 116 (2012): 985.
[20] H. Wu, F. Carotti, R. Gakham, N. Patel, and R. O. Scarlat, "Fluorination of Nuclear Graphite IG-110 in Molten 2LiF-BeF2 (FLiBe) Salt at 700 °C," *Journal of Fluorine Chemistry* 211 (2018): 159–170.
[21] L. Vergari and R. O. Scarlat, "The Impact of Neutron Irradiation, Oxidation and Fluorination on Tritium Uptake into and Desorption from Graphite in Molten Salts Environments," *Fusion Energy and Design* 168 (2021): 112627. https://doi.org/10.1016/j.fusengdes.2021.112627.
[22] E. Compare, S. Kirslis, E. Bohlmann, and F. Blankenship, *Fusion Product Behavior in the Molten Salt reactor Experiment*, ORNL-4865 (1977): 120–125.
[23] L. Jolivet, M. Leprince, S. Moncayo, L. Sorbier, C.-P. Lienemann, and V. Motto-Ros. "Review of the Recent Advances and Applications of LIBS-based Imaging." *Spectrochimica Acta Part B At. Spectrosc* 151(2018): 41–53. https://doi.org/10.1016/j.sab.2018.11.008.

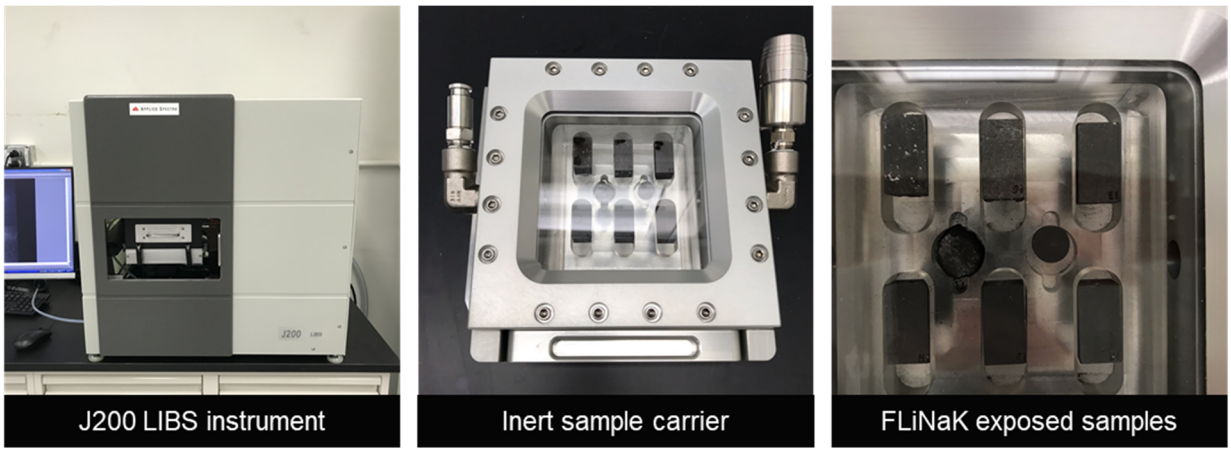

Figure 4. The LIBS instrument (left), sample holder (middle), and salt-exposed graphite specimens (right) loaded in the sealed sample holder.

Before proceeding to the systematic analysis of FLiNaK-impregnated graphite samples, a data collection and analysis methodology was established for future salt-graphite interaction studies. At this stage, the procedures for line intensity analysis and an unsupervised principal component analysis were explored separately and in combination for evaluation of LIBS data.

Figure 5 shows microscopy images of a FLiNaK-impregnated sample before and after the LIBS procedure. A lattice of 10 × 10 craters was created by laser beams during LIBS examination; the laser spot diameter was about 200 µm. The bottom panels show examples of single-spot spectra on clean graphite and salt-impregnated graphite. The spectral lines are easily identifiable for elements of interest (e.g., C, F, Li, Na, K, H, O).

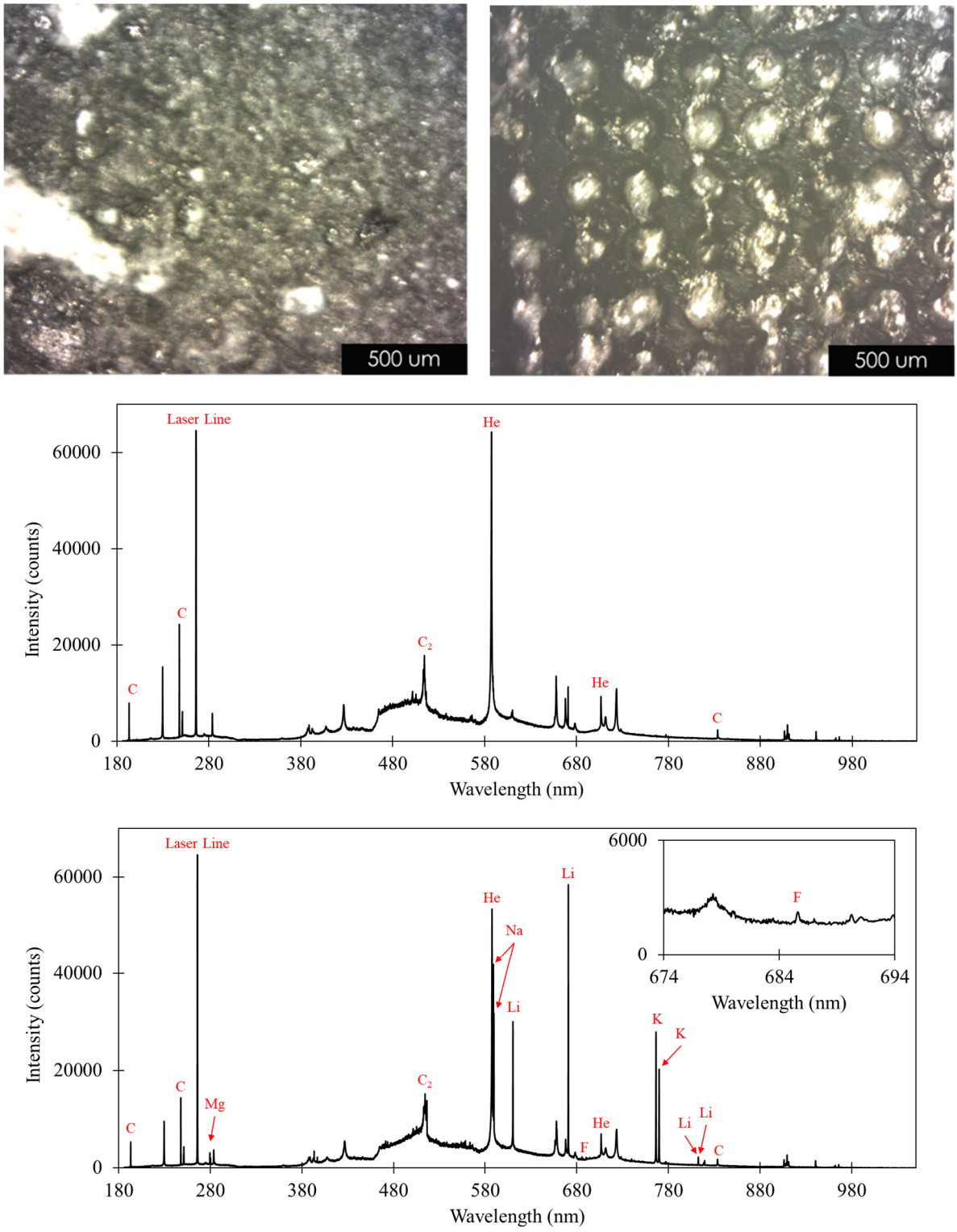

Figure 5. Optical microscopy images of graphite specimen's surface before and after examination by LIBS (top). Single-spot spectra of clean graphite surface not impregnated in salt (middle) and FLiNaK-impregnated graphite (bottom).

A correlation analysis of these results revealed a more complex behavior than initially expected. The results suggest that a reaction between FLiNaK and graphite might have occurred, which involved partitioning KF from the FLiNaK bulk. However, understanding this reaction will require further analysis of the data collected so far. The main achievement thus far was establishing a robust method for data collection and analysis. Future work will investigate chemical reactions through systematic analysis of FLiNaK-impregnated samples produced available from previous intrusion experiments. This analysis could benefit from using complementary techniques, such as Raman spectroscopy, which might confirm formation of fluorocarbon compounds.

2. EXPANDING FACILITIES FOR HANDLING FLiBe

The intrusion studies thus far were limited to FLiNaK. However, this year, an effort was initiated to expand the capabilities to add facilities where the team can conduct work with FLiBe.

Last year, the team successfully completed the installation of a three-glove inert gas glovebox. This glovebox is used for the welding of capsules that contain FLiBe. The glovebox is currently installed in Lab C-147 in Building 4500S. A picture of the installed glovebox is provided in Figure 6.

Figure 6. Installed and commissioned three-glove glovebox for welding Be-containing static capsules.

This year, a second intrusion test was built to handle FLiBe. A four-glove glovebox was procured, and another pressure vessel was built (Figure 7). The actual intrusion system design was modified to account for the limited head space within the glovebox. The FLiBe-dedicated pressure system will have similar temperature and pressure capabilities to the FLiNaK system, which is 750°C and 10 bar pressure. Enclosing the pressure system within the glovebox will eliminate the exposure of salt-intruded graphite samples to the atmosphere. The glovebox will also be equipped with a balance and a small optical microscope for direct imaging of the samples while in the glovebox.

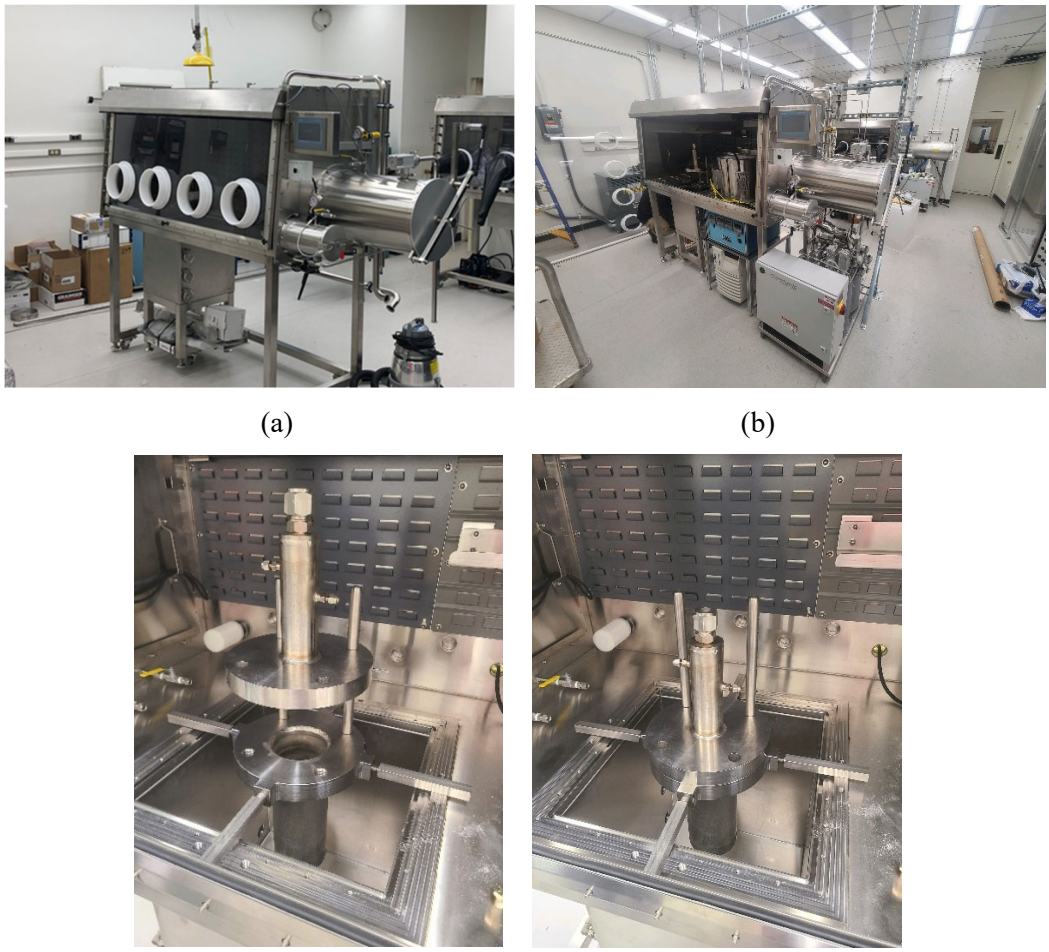

Figure 7. (a, b) New four-glove glovebox for intrusion system awaiting pressure vessel installation and (c, d) close-up photos of the pressure vessel being installed inside the glovebox.

3. GRAPHITE WEAR STUDIES IN MOLTEN SALTS

The circulation of fuel pebbles in the fluoride salt-cooled high-temperature reactor (FHR) reactor can produce graphite dust. If action is not taken to minimize pebble wear and dust production, then the graphite dust could be a concern for internal reactor components and might modify the operational parameters of the reactor itself. For the designer to take actions to mitigate dust generation and spreading through the reactor, proper measurements of wear resistance of graphite and fuel matrix components must be performed.[24]

To gain an initial fundamental understanding of the mechanical and chemical interactions between graphite pebbles in the molten salt environment, the team performed initial tribological measurements by using graphite extracted from pebble materials against stainless steel (SS) in dry Ar and in molten FLiNaK. The goal was to demonstrate the feasibility of tribological measurements in high-temperature molten FLiNaK and to determine the baseline for pebble graphite wear vs. dry SS. Future experiments will reproduce wear conditions in FHR by replacing the common standard steel base with a more realistic molten salt alloy (316H) and graphite materials (i.e., either nuclear graphite or pebble graphite).

3.1 EXPERIMENT AND MATERIALS

Friction and wear tests were performed in a molten FLiNaK at 650°C by using an Advanced Mechanical Technology Inc (AMTI) high-temperature tribometer (Figure 8) with modifications to accommodate the molten salt. Such a unique molten salt wear test was recently set up at ORNL and had already demonstrated the effectiveness and reliability of evaluating candidate bearing materials in molten chloride salt for concentrating solar power.[25,26] A pin-on-disc unidirectional sliding configuration was used to evaluate the tribological performance between a graphite pin (20 mm long with a radius of tip curvature of 20 mm) and a Type 316L SS square disc (25.4 × 25.4 mm). The graphite pins were machined from 40 mm diameter graphite pebbles by using wire electrical discharge machining. Each graphite pebble can provide two graphite pins, as shown at the top-right corner of Figure 8. The counterface was a Type 316L SS flat square of 25.4 × 25.4 × 1.6 mm. For each test, while in a glovebox, approximately 14 g of fluoride salt were loaded into the sample holder on top of the SS flat sample and sealed while still in a glovebox filled with dry Ar (bottom-right corner of Figure 8). To minimize the moisture and O contents, the sample holder was opened inside the test chamber that was pumped down and backfilled with dry Ar several times to ensure a dry, inert environment.

[24] J. J. Cogliati and A. M. Ougouag, "Pebble Bed Reactor Dust Production Model," HTR2008-58289, *Proceedings of the 4th International Topical Meeting on High Temperature Reactors*, September 28–October 1, 2008, Washington DC.
[25] X. He, R. Wang, D. Sulejmanovic, K. R. Robb, J. R. Keiser, K. Oldinski, and J. Qu, "Tribological Behavior of Ceramic-Alloy Bearing Contacts in Molten Salt Lubrication for Concentrating Solar Power," *Solar Energy Materials and Solar Cells* 225 (2021): 111065.
[26] X. He, K. R. Robb, D. Sulejmanovic, J. R. Keiser, and J. Qu, "Effects of Particle Size and Concentration of Magnesium Oxide (MgO) on the Lubricating Performance of a Chloride Molten Salt for Concentrating Solar Power," *ACS Sustainable Chemistry & Engineering* 9 (2021): 4941–4947.

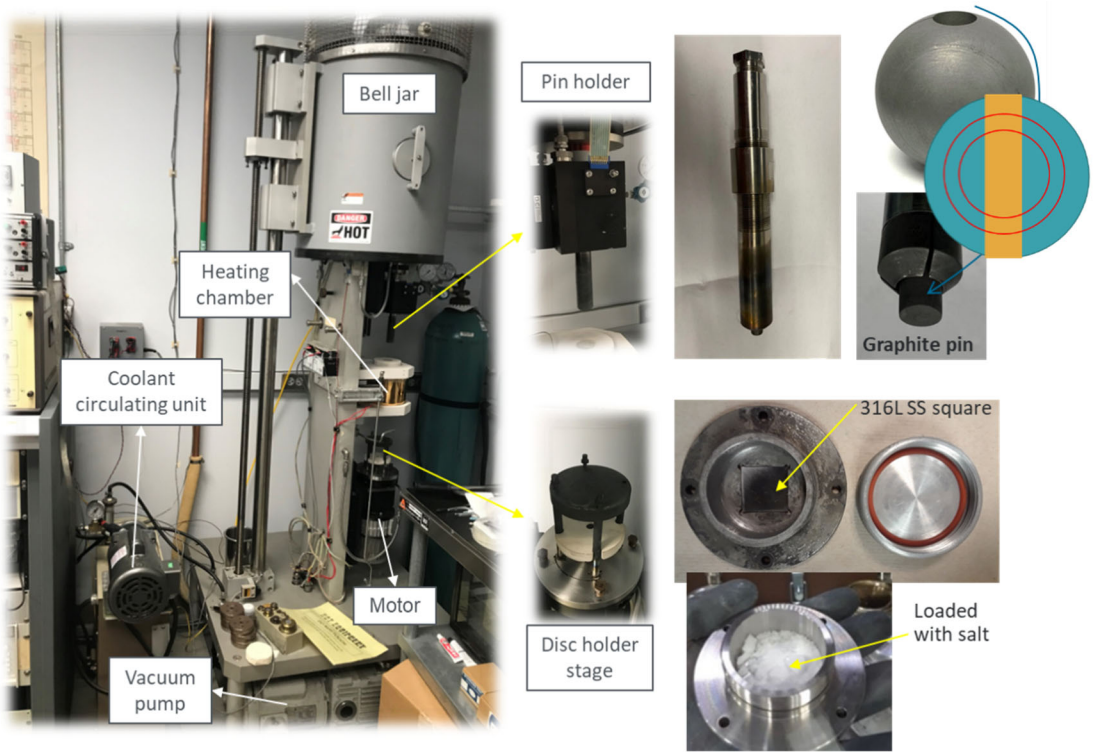

Figure 8. Experimental setup for wear testing of graphite in a FLiNaK molten salt.

For each test, a 0.111m/s (120 rpm, 17.7 mm diameter) sliding speed was used for a sliding distance of 1,000 m under a normal load of 20 N (~0.13 GPa initial Hertzian contact pressure). The friction force was measured in situ during the test. A water/sonication procedure was applied after each test to remove the salt residue on the specimens. Wear volumes of the graphite pin and SS square were quantified by using a Wyko NT9100 white light interferometer. A Hitachi S4800 scanning electron microscope (SEM) equipped with an energy dispersive spectroscopy (EDS) system was used to analyze the worn surface morphology and composition.

3.2 RESULTS AND DISCUSSION

The friction and wear results from the tests in dry conditions and in molten fluoride salt are summarized in Figure 9. The dry sliding test results are used as a baseline to understand the chemical (i.e., corrosion) and mechanical (i.e., lubrication) impacts of the molten salt. Two repeated tests were performed at each condition. In dry sliding, the graphite pin had wear loss (i.e., abrasion), whereas the SS square showed material deposition on the contact area instead. The deposit was later detected as C-based, likely material transfer from the graphite pin and accumulation of graphite wear debris. The volume of the deposit (~0.134 mm^3) on the SS square is about half of the wear volume of the graphite pin.

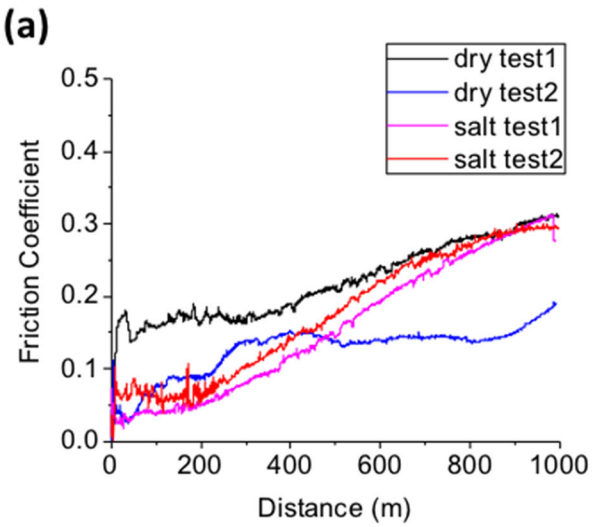

(b)

Wear volume (mm^3)	Pin	Disk
Dry test 1	0.32	(0.154)
Dry test 2	0.14	(0.113)
Average	$0.23^{\pm 0.09}$	$(0.134^{\pm 0.21})$
Salt test 1	0.29	0.057
Salt test 2	0.53	0.041
Average	$0.41^{\pm 0.12}$	$0.049^{\pm 0.008}$

** "( )" represents deposit*

Figure 9. (a) Friction coefficient traces of the graphite pin against 316L SS in dry and fluoride salt at 650°C; (b) wear volume on the pin and disc after cleaning.

In the case of sliding in the molten salt, the friction coefficients started at 0.05 and increased to ~0.27 at the end of the test. The initial value of friction coefficient was lower than that in dry sliding (~0.1), likely because the liquid salt at the pin-disc interface reduced adhesion. Unlike in dry sliding, the SS square had wear loss in the molten salt sliding as a result of a combination of abrasion and corrosion. The graphite pin wear in molten salt was higher than that in dry sliding, possibly because the wear-roughened SS surface became more abrasive and/or the graphite pin's mechanical properties degraded in molten salt.

Figure 10 presents the surface morphology and chemical composition of the wear scars on the graphite pin and SS square tested in dry sliding. Abrasive wear, microfracture, and a small amount of Fe particles (wear debris from the SS square) were observed on the graphite pin worn surface, as shown in Figure 10a. The SS square worn surface clearly shows parallel lines of deposit in the sliding direction, and the deposit was determined by EDS elemental mapping to be C dominant, as shown in Figure 10b. Such a graphite transfer film is believed to be wear protective in dry sliding.

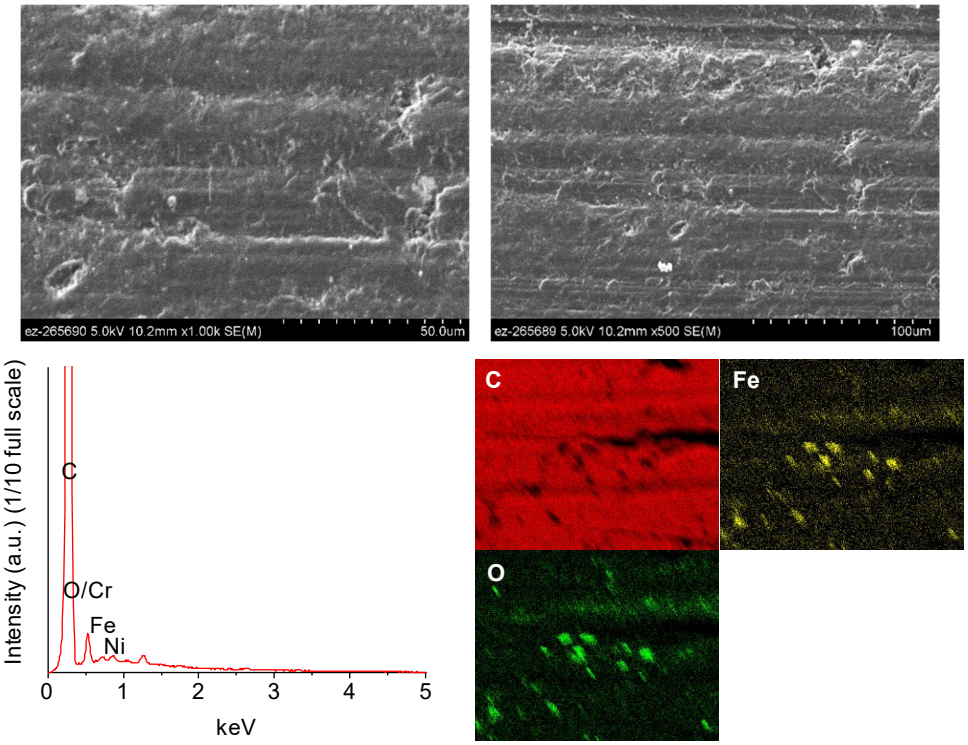

(a) Wear scar on graphite pin tested in dry sliding.

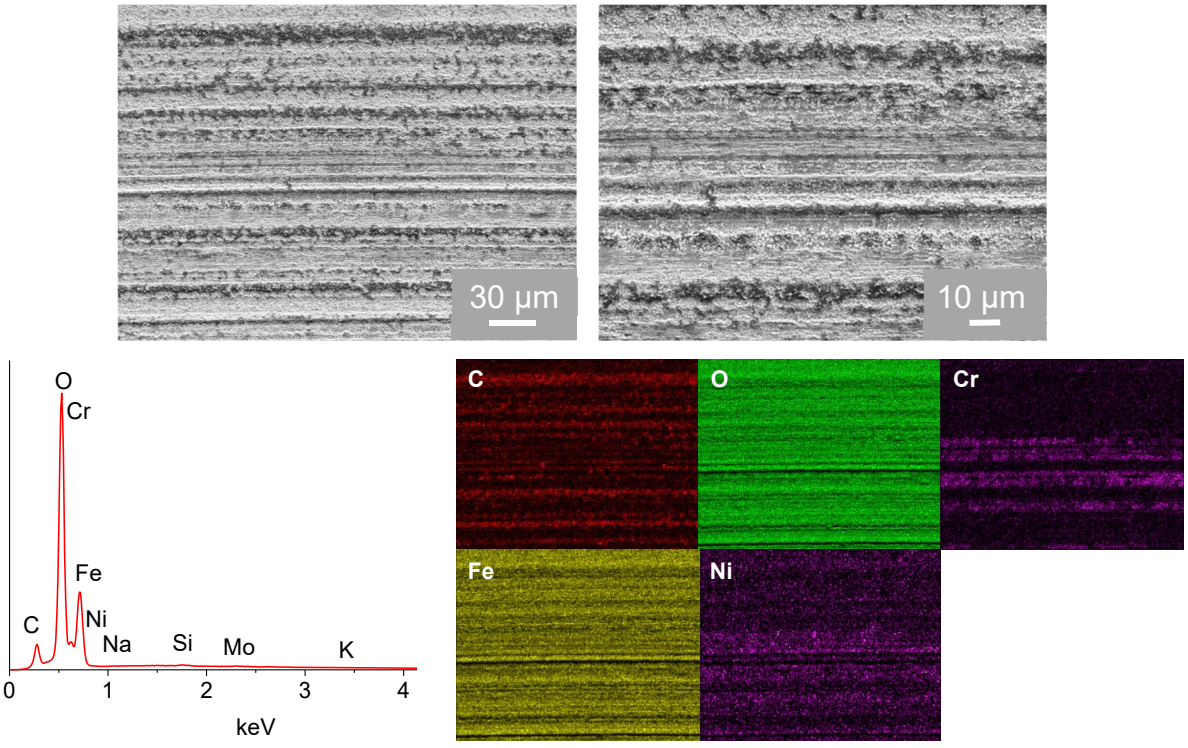

(b) Wear scar on 316L SS square tested in dry sliding.

Figure 10. SEM morphology examination and EDS chemical analysis of the worn surfaces on the (a) graphite pin and (b) SS square tested in dry sliding.

In comparison, Figure 11 shows the surface morphology and chemical composition of the wear scars on the graphite pin and SS square tested in molten salt. The graphite pin worn area had significantly more microfracture, which correlates to the increased wear loss compared with that in dry sliding. The reasons behind this could be the wear-roughened SS surface becoming more abrasive and/or the degradation of mechanical properties of the graphite surface in molten salt, which remain to be investigated. The SS square worn surface had both abrasion grooves and graphite deposit. After thorough cleaning in water sonication, the high F content on the SS wear scar indicates significant chemical reactions (i.e., corrosion) between the molten salt and the SS surface. The mechanical abrasion probably promoted corrosion by removing the corrosion products to expose the fresh metallic substrate and provide contact stress.

In next stage, the team will investigate the tribological performance of graphite sliding against Type 316H SS, a more realistic reactor alloy, in conditions more relevant to relative motions between graphite pebbles and the reactor molten salt container.

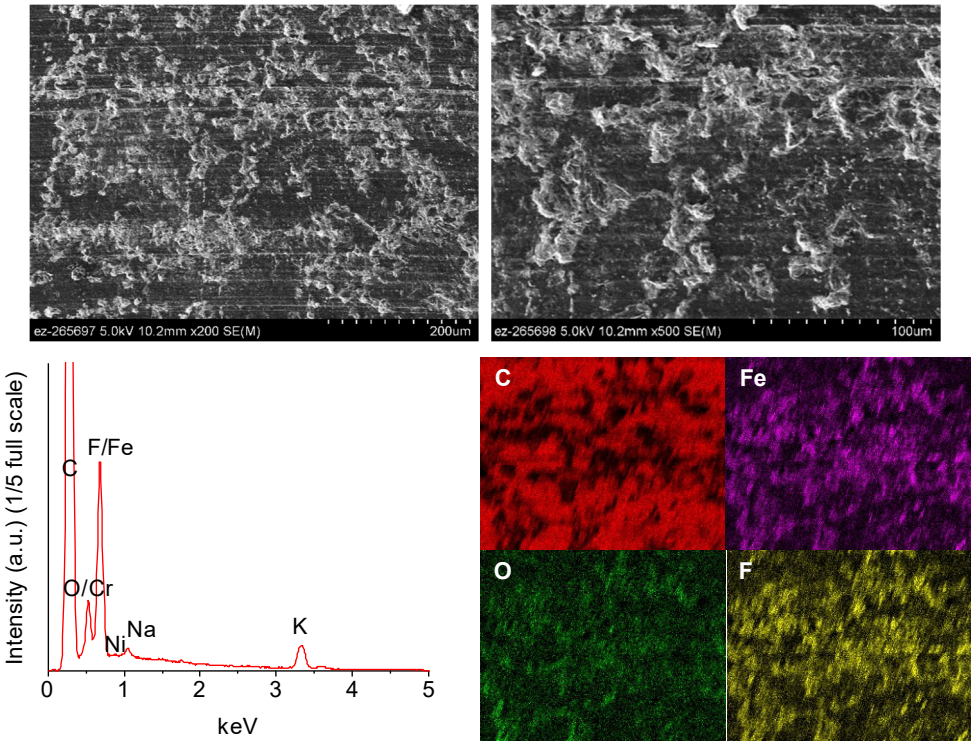

(a) Wear scar on graphite pin tested in molten salt.

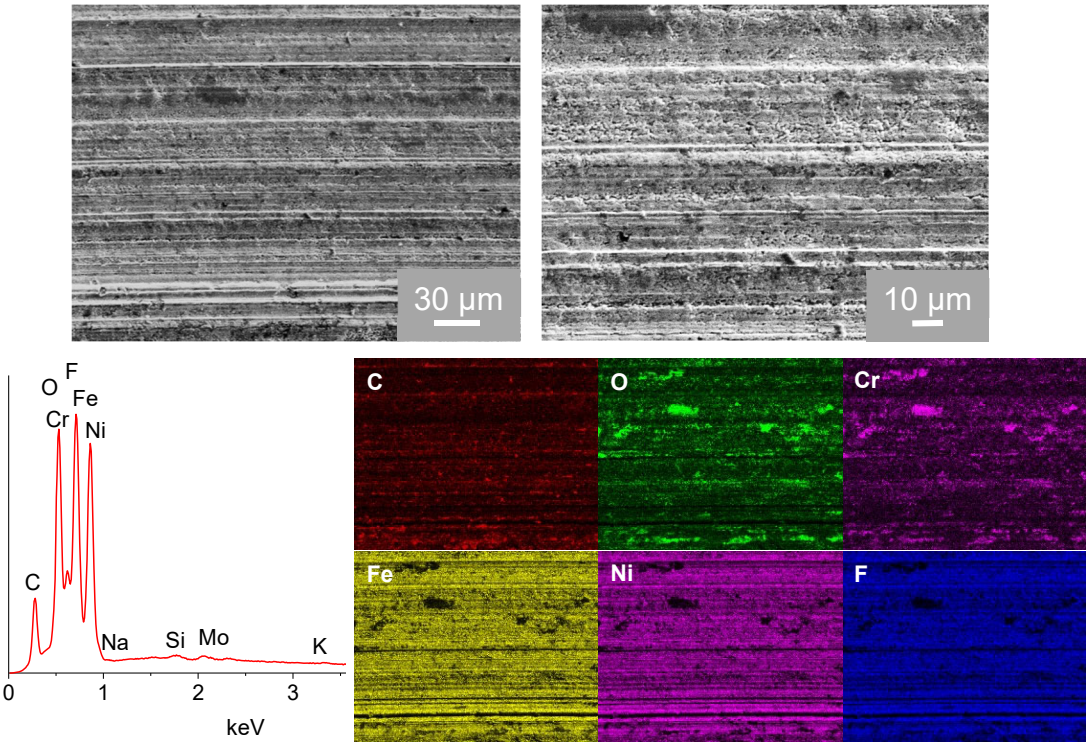

(b) Wear scar on 316L SS square tested in molten salt.

Figure 11. SEM morphology examination and EDS chemical analysis of the worn surfaces on the (a) graphite pin and (b) SS square tested in molten FLiNaK.

4. SUMMARY

This report summarized the activities performed in FY21 to investigate the interactions between nuclear graphite and molten salts, such as FLiNaK. First, building on last year's achievements, the team improved the procedure for measurements on pressurized salt intrusion in nuclear graphite and performed new experiments at variable pressures with specimens of different sizes and shapes. Additionally, the team actively provided suggestions and comments for ASTM D8091, *Standard Guide for Impregnation of Graphite with Molten Salts*, which came up for periodic revision in 2021. Second, the team expanded its capabilities to further characterize salt-impregnated graphite by procuring and installing a laser-induced breakdown spectroscopy (LIBS) instrument capable of producing a 3D chemical composition of a surface and subsurface region of specimens. A methodology for accurately analyzing information was developed, and a manuscript was submitted for publication. The LIBS instrument sample cell is sealed in controlled inert atmosphere, which is an advantage for using humidity-sensitive samples and Be-contaminated samples. This aligns with the team's effort to expand the capabilities of handling FLiBe and Be-containing materials in two newly installed glovebox units. Third, the team performed preliminary tribology tests for pebble graphite wear in contact with stainless steel in dry state and in molten salt at high temperature. These tests are needed to establish the baseline for the wear of pebble graphite by friction against metallic walls. The friction and wear of pebbles in the fluoride salt-cooled high-temperature reactor are expected to generate dust, which is a concern for other components' properties and safe reactor operation.